Langmuir
Letter
pubs.acs.org/Langmuir

Immobilization of Molecularly Imprinted Polymer Nanoparticles in Electrospun Poly(vinyl alcohol) Nanofibers

Silvia Piperno,[†,§] Bernadette Tse Sum Bui,[‡] Karsten Haupt,*[,‡] and Levi A. Gheber*[,†]

[†]*Avram and Stella Goldstein-Goren Department of Biotechnology Engineering, Ben-Gurion University of the Negev, Beer-Sheva 84105, Israel, and* [‡]*Compiègne University of Technology, UMR CNRS 6022, 60205 Compiègne, France.* [§]*Present address: Department of Materials and Interfaces, Weizmann Institute of Science, Rehovot 76100, Israel.*

Received October 13, 2010. Revised Manuscript Received December 10, 2010

We describe the fabrication of polymer nanofibers with entrapped molecularly imprinted polymer (MIP) nanoparticles and study their possible use in a fluorescence-based biosensor application. The MIP was imprinted with the fluorescent amino acid derivative dansyl-L-phenylalanine. Poly(vinyl alcohol) was used as a support for MIP nanoparticles because it is water-soluble and can be spun into very thin fibers. The fibers were characterized by atomic force microscopy and optical microscopy, and fluorescence microscopy was used for the characterization of target binding to the MIP. The fibers show close to 100% recovery upon extraction and rebinding of the target molecule. The selectivity of the system has been demonstrated through competitive binding experiments with nonfluorescent analogues boc-L-phenylalanine and boc-D-phenylalanine.

Introduction

Molecularly imprinted polymers (MIPs) are synthetic receptors obtained by the polymerization of suitable functional and cross-linking monomers around a molecular template.[1−3] Generally, the template is the target molecule later to be recognized and bound by the synthetic receptor or a closely related structural analogue. The functional monomers initially form a complex with the template, and following polymerization, their functional groups are held in position by the highly cross-linked polymeric network. Subsequent removal of the template reveals binding sites that are complementary in size, shape, and chemical functionality. In this way, a molecular memory is introduced into the polymer, which is now capable of selectively binding the target. Taking advantage of the higher physical and chemical stability of MIPs relative to that of biomacromolecules, it is anticipated that they can be more easily integrated into industrial fabrication processes. These properties make MIPs potentially very suitable as recognition elements for chemical sensors, biosensors, and biochips.[4] Moreover, for certain target analytes, MIPs as tailor-made synthetic receptors may be the only option because a natural receptor may not exist or may be difficult to obtain.

To use MIPs in applications such as sensing or affinity separation, it is often required to immobilize the polymer onto solid surfaces. This procedure usually results in a low surface area and leads to a relatively low binding capacity. A substantial increase in the surface area to volume ratio is obtained if MIPs are synthesized in the form of nanoparticles; however, their immobilization onto solid substrates is more difficult compared to their use in suspension. In this work, we report on the entrapping of MIP nanoparticles in electrospun polymer nanofibers, thus creating a nonwoven mat of sensing sites with a high surface area and accessibility.

Electrospinning is a method allowing the creation of polymer fibers with diameters in the range of a few tens of nanometers to a few micrometers.[5−7] During the past decade, this method has attracted much interest because of its simplicity and versatility. Starting with a polymer solution, it is possible to obtain microfibers or nanofibers that can be functionalized for a wide range of applications. A number of functional polymers, including polyaniline (a conductive polymer) and poly(vinylidene fluoride) (a piezoelectric polymer), have been directly spun.[6] Functional polymers of low molecular weight cannot be spun directly but can be blended with other polymers that are appropriate for electrospinning.[8] Electrospun fibers have been employed in various fields: mechanical engineering,[9−11] electrical engineering,[12−14] biomedical applications,[15−17] and sensing application.[18−20]

Combining MIPs with electrospun fibers is attractive, owing to the remarkable quality of the fibers such as their high surface area per unit mass, low cost, and easy inclusion of nanoparticles (NPs).

*Corresponding authors. E-mail: karsten.haupt@utc.fr, glevi@bgu.ac.il.

(1) Arshady, R.; Mosbach, K. *Makromol. Chem.* **1981**, *182*, 687–692.
(2) Wulff, G.; Sarhan, A. *Angew. Chem.* **1972**, *11*, 341.
(3) Zimmerman, S. C.; Lemcoff, N. G. *Chem. Commun.* **2004**, 5–14.
(4) Haupt, K. *Chem. Commun.* **2003**, 171–178.
(5) Huang, Z. M.; Zhang, Y. Z.; Kotaki, M.; Ramakrishna, S. *Compos. Sci. Technol.* **2003**, *63*, 2223–2253.
(6) Li, D.; Wang, Y. L.; Xia, Y. N. *Adv. Mater.* **2004**, *16*, 361–366.
(7) Teo, W. E.; Ramakrishna, S. *Nanotechnology* **2006**, *17*, R89–R106.
(8) Jin, H. J.; Fridrikh, S. V.; Rutledge, G. C.; Kaplan, D. L. *Biomacromolecules* **2002**, *3*, 1233–1239.
(9) Dror, Y.; Salalha, W.; Khalfin, R. L.; Cohen, Y.; Yarin, A. L.; Zussman, E. *Langmuir* **2003**, *19*, 7012–7020.
(10) Huang, Z. M.; Zhang, Y. Z.; Ramakrishna, S.; Lim, C. T. *Polymer* **2004**, *45*, 5361–5368.
(11) Ko, F.; Gogotsi, Y.; Ali, A.; Naguib, N.; Ye, H. H.; Yang, G. L.; Li, C.; Willis, P. *Adv. Mater.* **2003**, *15*, 1161.
(12) Ahn, Y. R.; Song, M. Y.; Jo, S. M.; Park, C. R.; Kim, D. Y. *Nanotechnology* **2006**, *17*, 2865–2869.
(13) Chronakis, I. S.; Grapenson, S.; Jakob, A. *Polymer* **2006**, *47*, 1597–1603.
(14) Kim, J. R.; Choi, S. W.; Jo, S. M.; Lee, W. S.; Kim, B. C. *Electrochim. Acta* **2004**, *50*, 69–75.
(15) Pham, Q. P.; Sharma, U.; Mikos, A. G. *Tissue Eng.* **2006**, *12*, 1197–1211.
(16) Schiffman, J. D.; Schauer, C. L. *Polym. Rev.* **2008**, *48*, 317–352.
(17) Venugopal, J.; Zhang, Y. Z.; Ramakrishna, S. *J. Nanoeng. Nanosyst.* **2004**, *218*, 35–45.
(18) Ding, B.; Kim, J. H.; Miyazaki, Y.; Shiratori, S. M. *Sens. Actuators, B* **2004**, *101*, 373–380.
(19) Piperno, S.; Passacantando, M.; Santucci, S.; Lozzi, L.; La Rosa, S. *J. Appl. Phys.* **2007**, *101*, 124504.
(20) Sawicka, K.; Gouma, P.; Simon, S. *Sens. Actuators, B* **2005**, *108*, 585–588.

In addition, the nonwoven mat created by the fibers provides easy access to the target molecules. Cronakis and colleagues[21−24] have already used this approach for MIPs specific to theophylline, 17β-estradiol, and propranolol by including them in poly(ethylene terephthalate) nanofibers.

In the present work, as a first step toward biological applications (requiring water-compatible materials), we tested the feasibility of including MIP nanoparticles in poly(vinyl alcohol) (PVA) nanofibers by electrospinning. PVA is a biocompatible polymer[25] and it can be spun in water. Because it contains free hydroxyl groups, it can be easily cross linked to stabilize the fibers. Moreover, PVA can be spun in relatively thin fibers that do not block access to the entrapped MIP NPs. It is thus a good candidate for a matrix in future MIP-NP biosensors and for other applications in the biomedical field such as affinity filtration and slow drug release. As a model target, we used the fluorescent amino acid derivative dansyl-L-phenylalanine (dansyl-L-Phe). The fibers were characterized morphologically by atomic force microscopy and optical microscopy. The binding of the target molecule and other related molecules to the fibers was characterized by fluorescence microscopy.

Experimental Section

Chemicals. Poly(vinyl alcohol) (98%, M_w = 13 000−23 000), sodium hydroxide (>98%), 1,4-butanediol diglycidyl ether (95%), methacrylic acid (MAA), 4-vinylpyridine (4-VPy), ethylene glycol dimethacrylate (EDMA), dansyl-L-Phe, boc-L-Phe, and boc-D-Phe were purchased from Sigma-Aldrich. Sodium borohydride (95%) was purchased from Riedel De Haen. Analytical-grade acetonitrile, methanol, and ethanol were from Bio-Lab LTD (Jerusalem, Israel). Acetic acid was from Frutarom (Haifa, Israel). Azo-bis-dimethylvaleronitrile (Vazo-52, ABDV) was purchased from DuPont. 4-VPy was distilled under vacuum before use and kept at −20 °C in the dark.

Synthesis of MIP and NIP Nanoparticles. Dansyl-L-Phe MIP nanoparticles were synthesized by adapting a protocol developed by Kriz et al.[25] for precipitation polymerization. A template (0.1 mmol, dansyl-L-Phe), 4-VPy (0.4 mmol, 43 μL), MAA (0.4 mmol, 34 μL), EDMA (4 mmol, 755 μL), and ABDV (0.04 mmol, 9 mg) were dissolved in 10 mL of anhydrous acetonitrile in a glass vial fitted with an airtight septum. The mixture was cooled on ice and purged with nitrogen for 5 min and then left to polymerize overnight at 40 °C in a water bath. A white precipitate was obtained. CH_3CN (5 mL) was added, and the mixture was subjected to ultrasonication until a homogeneous suspension was obtained. The polymer suspension was centrifuged (19 000 rpm, 30 min) and successively washed with four rounds of methanol/acetic acid (4/1), followed by three rounds of ethanol/acetic acid (4/1) (1 h on a shaker at 60 °C) until no fluorescence was detected in the washing solutions. The nanoparticles were then incubated three more times for 1 h at 60 °C in methanol. After centrifugation, the polymers were dried overnight under vacuum. Particles with a diameter of 400 nm were obtained, as determined by dynamic light scattering using a Zetasizer Nano-ZS (Malvern Instruments, Orsay, France). Nonimprinted polymers (NIPs) were synthesized under the same conditions but without the addition of template and processed identically to the MIPs, and their dimensions were similar.

Batch Equilibrium Binding Studies. The imprinted and nonimprinted particles were suspended in anhydrous acetonitrile in a sonicating bath. From this stock suspension, polymer concentrations ranging from 0.25 to 3 mg/mL were pipetted into 2 mL polypropylene microcentrifuge tubes and 250 nM dansyl-L-Phe was added. The final volume was adjusted to 1 mL with acetonitrile. The tubes were wrapped in aluminum foil and incubated overnight at ambient temperature on a tube rotator (SB2, Stuart Scientific). The polymer particles were centrifuged at 16 000g for 15 min, and the fluorescence (λ_{ex} = 340 nm; λ_{em} = 520 nm) of the supernatant (700 μL) was measured using a Cary Eclipse spectrofluorimeter (Varian). The amount of dansyl-L-Phe bound to the polymers was calculated by subtracting the amount of unbound dansyl-L-Phe from the initial amount of dansyl-L-Phe added to the mixture.

Electrospinning. MIP NPs were suspended in an H_2O/ethanol 7:3 (v/v) blending solvent by sonication, and then poly(vinyl alcohol) was dissolved in the suspension. The MIP/PVA ratio was 1:30 (w/w). To dissolve the PVA, the solution was heated on a hot plate at 80 °C for 10 min and then sonicated again to disperse the particles. We found that 30% solid (w/v) in the solvent mixture yielded the appropriate viscosity for electrospinning.

The solution was loaded into a 1 mL disposable syringe with a 23 gauge needle. A glass microscope slide (Menzel GmbH, Germany) was used as a substrate and was positioned 15 cm away from the tip of the needle. Electrospinning was performed at 20 kV using a vertical setup.

Cross Linking of Electrospun Fibers. The fibers were incubated for 8 h in a 1:1 mixture of butanediol diglycidyl ether and 0.6 M NaOH containing 50 mM $NaBH_4$, under shaking, followed by washing with water.[26]

Microscopic and Binding Analyses of Fibers. The composite fibers were imaged by AFM (Nanonics NSOM/AFM 100) and optical microscopy (ZEISS-Axioplan2). Binding of the target molecule to the fibers was studied by fluorescence microscopy using a Dansyl filter set from Chroma (D350_50x as the excitation filter, 400CLP as the dichromatic mirror, and E420LPv2 as the emission filter). Dansyl-L-Phe was dissolved in acetonitrile at different concentrations in the range between 10 μM and 1 mM and incubated with MIP fibers in a total volume of 15 mL on a rocking table for 4 h at room temperature. The fluorescence of the entrapped NPs was analyzed by quantifying 20 spots in each of five different regions of the sample (100 measurements in total) for each target concentration. The average intensity (total counts divided by the total number of pixels) for each NP was calculated and reported. The background was assessed from the areas of the images that did not contain fibers (and NPs) and was subtracted from the values obtained for the NPs.

Results and Discussion

MIP nanoparticles imprinted with dansyl-L-Phe were first tested in batch equilibrium binding assays with fluorescence detection in the supernatant. The binding to the MIP increased with polymer concentration, yielding a hyperbolic curve with saturation (Figure 1a). Binding to the NIP also increased with polymer concentration but to a much lesser extent, indicating a good imprinting effect. No nonspecific binding was detected up to 500 μg of polymer/mL. To determine the selectivity of the MIP, competition studies at equilibrium were performed with nonfluorescent boc-L-Phe and boc-D-Phe as competing ligands. Fixed amounts of 0.5 mg/mL of MIP and 250 nM dansyl-L-Phe and variable amounts of competitors ranging from 0.1 to 8000 μM were tested (Figure 1b). The values of IC_{50} (the concentration of competing ligands required to displace 50% of dansyl-L-Phe) for boc-L-Phe and boc-D-Phe, determined from a nonlinear regression fit, were 127 and 500 μM, respectively. This means that the

(21) Chronakis, I. S.; Jakob, A.; Hagstrom, B.; Ye, L. *Langmuir* **2006**, *22*, 8960–8965.
(22) Chronakis, I. S.; Milosevic, B.; Frenot, A.; Ye, L. *Macromolecules* **2006**, *39*, 357–361.
(23) Yoshimatsu, K.; Ye, L.; Lindberg, J.; Chronakis, I. S. *Biosens. Bioelectron.* **2008**, *23*, 1208–1215.
(24) Yoshimatsu, K.; Ye, L.; Stenlund, P.; Chronakis, I. S. *Chem. Commun.* **2008**, 2022–2024.
(25) Kriz, D.; Ramstrom, O.; Svensson, A.; Mosbach, K. *Anal. Chem.* **1995**, *67*, 2142–2144.
(26) Sundberg, L.; Porath, J. *J. Chromatogr.* **1974**, *90*, 87–98.

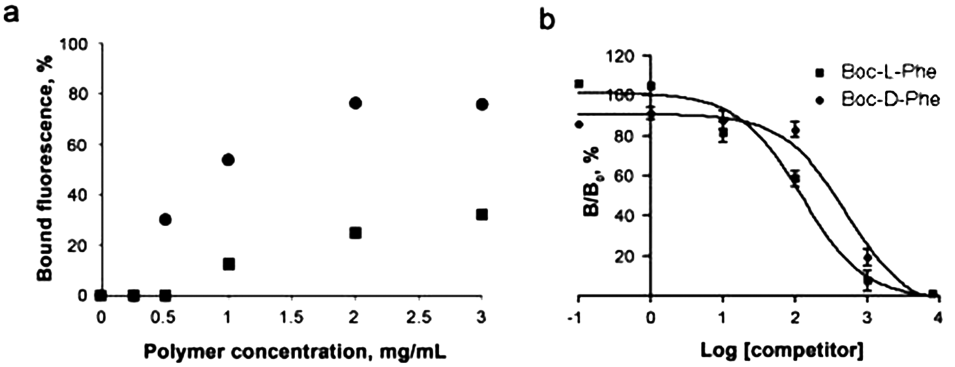

Figure 1. (a) Equilibrium binding isotherms for dansyl-L-Phe (250 nM) on MIP (●) and NIP (■) in acetonitrile. Data are the means of duplicate experiments from two different batches of polymers. (b) Inhibition of dansyl-L-Phe binding (250 nM) to MIP at 0.5 mg/mL by boc-L-Phe (■) and boc-D-Phe (●) in acetonitrile. B/B_0 is the ratio of the amounts of dansyl-L-Phe bound in the presence and absence of a displacing ligand. Data are the means of triplicate experiments. The error bars represent standard deviations.

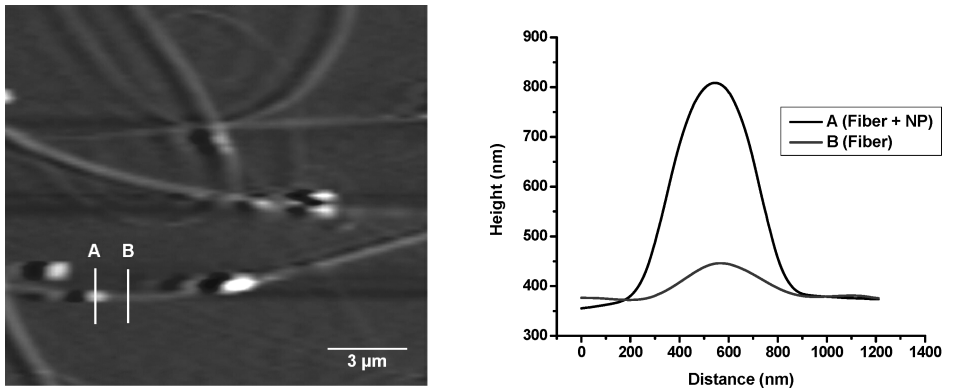

Figure 2. (Left) Contact-mode AFM image of PVA fibers with immobilized MIP NPs. (Right) Height profile along the lines in the AFM image. The fiber diameter is ~100 nm, and the NP diameter is ~400 nm.

cross reactivity of the D enantiomer with respect to that of the L enantiomer is 25%, indicating the good enantioselectivity of the polymer. The fact that 127 μM boc-L-Phe is needed to displace 250 nM dansyl-L-Phe again confirms the selectivity of the MIP.

Preparation of the Fibers: The Electrospinning Process. PVA-based fibers were not stable in the solvents used for the binding assays and for the regeneration of the MIP fibers (acetonitrile and methanol−acetic acid). This problem was solved by cross linking the fibers with butanediol diglycidyl ether. Figure 2 shows an AFM image of PVA fibers with NPs immobilized along them. An analysis of the images yields fiber diameters in the range of 80−350 nm. The purpose of fibers with diameters smaller than those of the nanoparticles is to avoid complete coverage of the embedded NPs. On the contrary, a large part of the NP surface should protrude beyond the surface of the fiber to increase the accessibility of the target molecules to the cavities in the NP. Indeed, the AFM image in Figure 2 shows that this is the case: the diameter of the fiber along the line marked B is ~100 nm, and the diameter along the line marked A (a section of the NP and the fiber) is ~400 nm. The shadows appearing to the left of the features in Figure 2 are a result of feedback overshoot (in the fast scan direction), but the artifact was avoided by taking height profiles in the perpendicular (vertical) direction, as indicated by white lines (A and B) in the figure.

Target binding to the MIP-PVA composite fibers was then studied by fluorescence microscopy, comparing the bright-field image and the image acquired in fluorescent mode and overlaying both images. As a result, fluorescence appears only in the proximity of the NPs. Thus, we observe no nonspecific binding of the target (dansyl-L-Phe) to the fibers. An example of such images is shown in Figure SI1 of the Supporting Information.

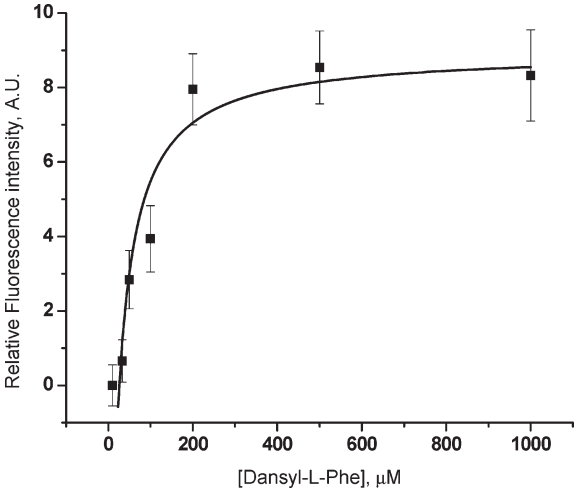

Figure 3. Background-normalized binding of dansyl-L-Phe to MIP-PVA nanofibers as a function of concentration. The fit represents a Langmuir binding isotherm with $K_D = 21 \pm 5$ μM. Fluorescence intensity measurements were made in triplicate, and the error bars represent the standard deviation.

A binding isotherm was then recorded in acetonitrile by varying the concentration of dansyl-L-Phe from 10 μM to 1 mM, yielding a curve that indicates saturation and thus a limited number of binding sites, which is typical for affinity binders such as

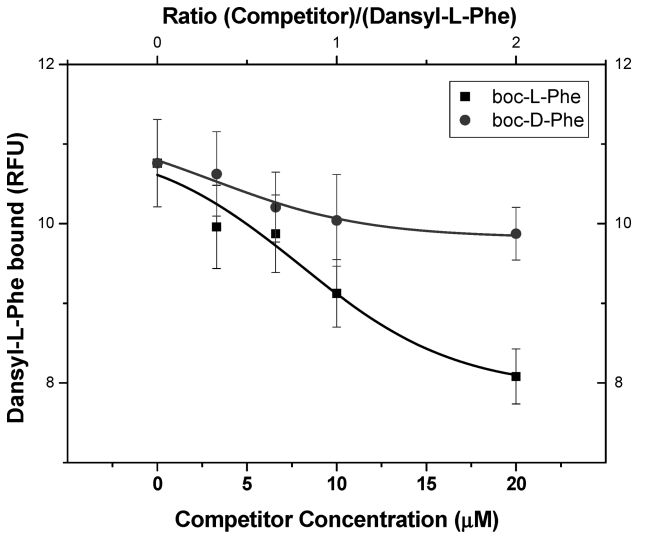

Figure 4. Competitive binding analysis. Binding of dansyl-L-Phe (10 μM) in the presence of increasing concentrations of boc-L-Phe and boc-D-Phe. The competitor/dansyl-L-Phe ratio is indicated on the upper horizontal axis. Fluorescence intensity measurements were made in triplicate, and the error bars represent the standard deviation.

MIPs (Figure 3). The curve was fit with a Langmuir isotherm equation with one class of binding sites of the form $I = I_{max}(c/(K_D + c))$, where I is the fluorescence intensity, c is the concentration of dansyl-L-Phe, and K_D is the dissociation constant. To obtain a meaningful fit consistent with the Langmuir isotherm assumption (zero binding at zero ligand concentration), the lowest intensity obtained (ligand that could not be extracted) was set to zero. The absolute lowest values can be read in Figure SI2 in the Supporting Information. The fit yields $K_D = 21 \pm 5\ \mu$M.

To check that the binding is reversible, a number of successive binding experiments were performed at a dansyl-L-Phe concentration of 1 mM. Between binding cycles, the fibers were regenerated by incubation in methanol/acetic acid (4:1) for 4 h, followed by washing with pure methanol three times for 20 min each. As a result, very reproducible fluorescence intensities were obtained after the different binding experiments and after the washing steps (Figure SI2 in the Supporting Information). This fact, together with Figure SI1 where it is shown that the fluorescence signal originates in the NPs only, demonstrates the good accessibility of the binding sites on the NPs.

To test for selectivity and confirm the imprinting effect, competitive binding experiments were performed using the two enantiomers of a nonfluorescent analogue of dansyl-phenylalanine as competitors. The fibers were incubated with a fixed concentration of dansyl-L-Phe (10 μM) in the presence of varying concentrations of nonfluorescent boc-L-Phe or boc-D-Phe (Figure 4). It is expected that boc-L-Phe, having the same chiral conformation as dansyl-L-Phe, will compete with the binding of the latter, whereas the opposite enantiomer, boc-D-Phe, will not compete or will compete to a lesser extent. The measurements show a decrease in the fluorescence signal with increasing boc-L-Phe concentration as a result of the competition for the dansyl-L-Phe binding sites. However, when boc-D-Phe was used as the competitor, a markedly weaker competition was observed. This demonstrates the enantioselectivity of the MIP-PVA nanofibers and at the same time confirms the imprinting effect. The curves represent fitting to a one-site competition model according to the equation $y = A_2 + ((A_1 - A_2)/(1 + 10^{(x - \log x_{0.5})}))$, where A_1 and A_2 are the upper and lower asymptotes, respectively, x is the competitor concentration, and $x_{0.5}$ is the competitor concentration for which half of the target is displaced by the competitor (IC50). The curves serve as a guide to the eye.

Conclusions

In this work, dansyl-LPhe MIP nanoparticles have been immobilized on electrospun PVA fibers. We show that PVA yields relatively thin fibers, allowing the entrapping of MIP particles with diameters larger than those of the fibers. This allows a large portion of the NP surface to be exposed and accessible to the target molecule. Additionally, PVA is a biocompatible polymer and can be spun in water. It can thus be used as a support for MIPs that are to be used in aqueous environments. Binding experiments, using fluorescence quantification, show that NPs embedded in electrospun PVA fibers preserve the reversible and selective binding properties as well as the recovery after washing.

Acknowledgment. We gratefully acknowledge financial support from the European Union via the Marie-Curie Research Training Network NASCENT (MRTN-CT-2006-033873)

Supporting Information Available: Light microscopy images of fibers with NPs embedded and repeated binding experiment quantification. This material is available free of charge via the Internet at http://pubs.acs.org.